reported to be involved in lymphocyte migration in cell adhesion during colonization of the thymus by hematopoietic precursor cells, and also has pantetheinase activity (Pitari *et al.*, 2000). Though vanin 1 is not reported to play a role in lipid metabolism so far, it was in fact reported to be an inducible gene by PPARα (Yamazaki *et al.*, 2002).

CD36 antigen (fatty acid translocase (FAT)) is involved in regulating the uptake of fatty acid across the plasma membrane (Bonen *et al.*, 2004) and also reported to be induced by PPARα agonists in liver (Motojima *et al.*, 1998). Moreover, it has been reported that CD36 plays a role in plasma TG homeostasis via modulation of LPL activity (Goudriaan *et al.*, 2005). Thus, an increase of this gene expression would be one of the mechanisms of plasma TG level decrease in the corresponding animal.

A previous report described that CIDEA-null mice presented TG decrease in fasting condition compared with wild type (Zhou *et al.*, 2003). Because expression of the CIDEA gene was up-regulated in liver treated with TG-decreasing compounds in both principal components (data not shown), it seemed to be a compensatory reaction. In addition, compounds with large PC 2 values, i.e., WY, GFZ, CFB and BBr, are reported to be agonists of PPARα (Kunishima *et al.*, 2003; van Raalte *et al.*, 2004). Activation of PPARα induces hepatic gene expression by β-oxidation of fatty acid and hydrolysis of TG-rich lipoprotein via activation of peripheral lipoprotein lipase (LPL) (van Raalte *et al.*, 2004). In addition to activation of fatty acid β-oxidation, PPARα inhibits de novo fatty acid synthesis in liver (Schoonjans *et al.*, 1996). In peripheral tissue, it has also been reported that gene expression of APOC3 (a natural inhibitor of LPL activity) decreases by PPARα and subsequently LPL activity is increased (Staels *et al.*, 1995). Taken together, these results suggest that the trend of increasing PC 2 is linked to lowering plasma TG level via PPARα activation.

"Glutathione *S*-transferase A5", "aldehyde dehydrogenase family 1, member A1", "liver UDP-glucuronosyltransferase, phenobarbital-inducible form", "carbonic anhydrase 2", "cytochrome P450, family 2, subfamily b, polypeptide 15" had smaller eigenvector values for PC 2 (Table 5). They (except carbonic anhydrase 2) have been reported to be constitutive androstane receptor (CAR)-inducible genes (Kakizaki *et al.*, 2003). Although there is no report that PTU, OPZ, TAA, MP, SS and CMA activate CAR so far, the present results suggested that these compounds could

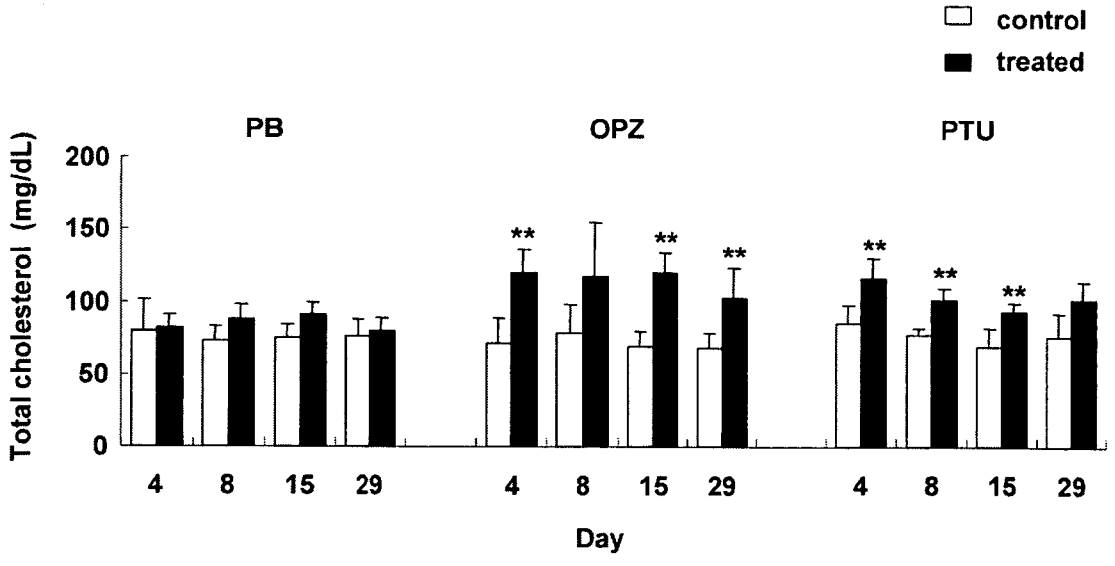

Fig. 3. Effects of PB, OPZ, PTU on plasma total cholesterol level.
Plasma total cholesterol concentrations were estimated as described in materials and methods. Open (control) and filled (treated) columns represent total plasma cholesterol concentration. Values are expressed as mean ± SD of 5 rats for each time and compound. Significant difference from control rat: (*$p<0.05$, **$p<0.01$: Dunnett test).

induce the same xenobiotics metabolizing enzymes as PB does (Kakizaki *et al.*, 2003). Meanwhile, these enzymes (such as UDP-glucuronosyltransferase) are able to metabolize not only xenobiotics but also serum thyroid hormone (TH) (Qatanani and Moore, 2005), which has a role in comprehensive regulation of energy metabolism (Weiss *et al.*, 1998). It has been reported that rats with hypothyroidism induce and activate peripheral lipoprotein lipase (LPL), the key enzyme in hydrolysis of TG-rich lipoproteins, such as chylomicron and VLDL (Kern *et al.*, 1996; Ong *et al.*, 1994). In fact, it has also been reported that PB, PTU and OPZ are able to alter blood TH level (Masubuchi *et al.*, 1997; De Sandro *et al.*, 1991). CAR is also activated by caloric restriction (Maglich *et al.*, 2004). With depletion of food, the body needs to lower its energy requirement. It might be possible that CAR was activated in rats whose food consumption was decreased (Fig. 1). Thus, identified probe sets might be indirectly related to plasma TG decrease via reduction of blood TH by CAR activation in at least two ways. Accordingly, the feature in decreased PC 2 value could be related to lowering plasma TG level via CAR activation. Moreover, it has been reported that TH is a physiological regulator of cholesterol metabolism (Weiss *et al.*, 1998; Gullberg *et al.*, 2000, 2002; Hashimoto *et al.*, 2006; Ness and Chambers, 2000) and hypercholesterolemia is found in patients with hypothyroidism (Diekman *et al.*, 2000). It was also noted in the present study that total cholesterol levels in OPZ and PTU with smaller PC 2 values were found to be increased (Fig. 3). These indirect evidences also supported the assumption that TH levels were involved in plasma TG reduction.

As shown in Table 6, genes with smaller eigenvector values for PC 1 such as "aldehyde dehydrogenase A5", "glutathione *S*-transferase A5", "vanin 1", "carboxylesterase 2" and "CD36 antigen" were important genes that contribute to shift each sample to either direction of PC 2. It appears that PC 1 shows a lowering of plasma TG level via either or both of two mechanisms (PPARα and/or CAR activation). Interestingly, AM had small PC 1 values, while near zero in PC 2. This result is supported by previous reports that AM induces the expression of PPARα target genes (McCarthy *et al.*, 2004) and lowers serum TH level (De Sandro *et al.*, 1991). Thus, these two directions might have been balanced in the case of the plasma TG reduction by AM.

It was previously reported that PPARα was also activated by fasting (Kersten *et al.*, 1999; Lee *et al.*, 2004; Leone *et al.*, 1999), as well as by CAR. An interesting question is why these 218 probe sets classify the compounds with various pharmacological and toxicological properties based on their different mechanisms. Genes with the largest or smallest eigenvector values for PC 2 such as vanin 1 and glutathione *S*-transferase A5 are related to each nuclear receptor, PPARα and CAR, respectively, rather than to plasma TG homeostasis. CD36, which was involved in regulating the uptake of fatty acid, mainly contributed to PC 1. This means that CD36 could be an important gene directly related to plasma TG level, while its background mechanisms are represented by genes like vanin 1 or glutathione *S*-transferase A5. Thus, we considered that these probe sets work to classify the compounds by PCA, based on each nuclear receptor-mediated TG-lowering mechanism.

In the present study, some compounds such as ANIT, CCL4 and INAH were not dispersed in PCA, suggesting potential involvement of other TG-decreasing mechanism(s). Because the plasma TG level is influenced by the balance of intake from diet, hepatic synthesis, secretion from liver, and metabolism at peripheral tissues, many factors remain to be investigated. Moreover, since it has been reported that the action of TH on LPL activity is in the opposite direction between human and rat (Kern *et al.*, 1996; Ong *et al.*, 1994), it is necessary to elucidate the species difference in the mechanism of plasma TG decrease.

In conclusion, we identified 218 probe sets from gene expression profiles in liver treated with various TG-decreasing compounds stored in our database. Analysis of identified probe sets suggested two mechanisms in plasma TG decrease, i.e., PPARα and CAR activation, in addition to at least one unknown mechanism. The proposed mechanisms of lowering plasma TG level elucidated by the present study are summarized and depicted in Fig. 4. Further studies, especially verifying experiments, are clearly necessary to confirm our hypothesis and to establish useful biomarker genes. The presently extracted probe sets could be a source of potential biomarkers for development of a novel hypolipidemic agent and/or interpretation of the mechanism of plasma TG reduction.

ACKNOWLEDGMENT

We thank Nami Asari, Seiko Ueda, Chiaki Kondo, Shogo Hayakawa, Yasunori Suzuki, Izumi Yumita, Hayato Fukusumi and Seiko Ohta (Toxicogenomics Project in Japan) for analyses of liver gene

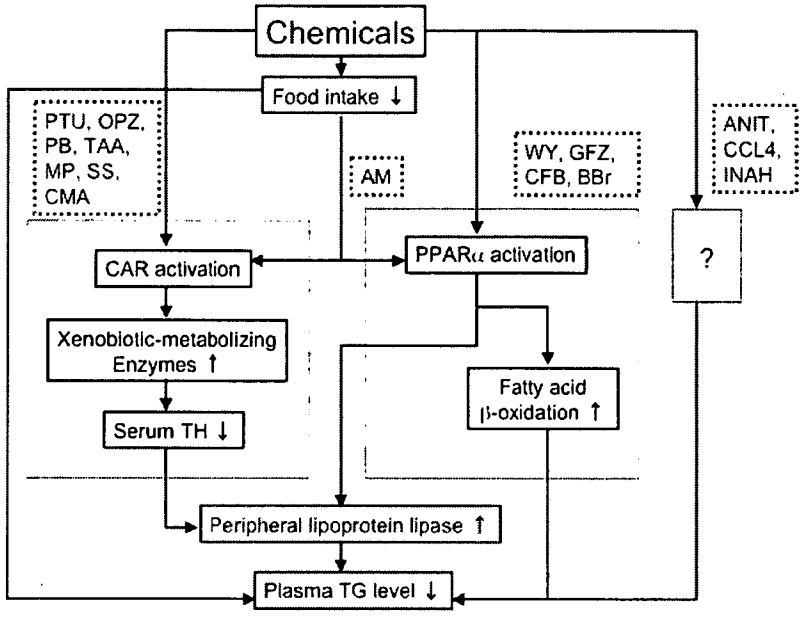

Fig. 4. Proposed TG-decreasing mechanisms of various drugs elucidated by comprehensive gene expression analysis.
Intake of chemicals induces direct or indirect CAR and/or PPARα activation. CAR activation leads to induction of hepatic xenobiotic-metabolizing enzymes, which reduces the serum thyroid hormone (TH) level. PPARα activation leads to hepatic induction of fatty acidβ-oxidation. Both of the nuclear receptor activations increase peripheral lipoprotein lipase activity, which subsequently lowers the plasma TG level. PTU, OPZ, PB, TAA, MP, SS, and CMA are CAR activators, whereas WY, GFZ, CFB, and BBr are PPARα activators. AM appears to have both properties to the same extent. There must be other mechanism(s), since ANIT, CCL4, and INAH, which showed obvious TG-decreasing effects, could not be differentiated by the present analysis.

expression. This study was supported in part by a grant from the Ministry of Health, Labor and Welfare (H14-Toxico-001).

REFERENCES

Bock, K.W., Lipp, H.P. and Bock-Hennig, B.S. (1990): Induction of drug-metabolizing enzymes by xenobiotics. Xenobiotica, **20**, 1101-1111.

Bonen, A., Campbell, S.E., Benton, C.R., Chabowski, A., Coort, S.L., Han, X.X., Koonen, D.P., Glatz, J.F. and Luiken, J.J. (2004): Regulation of fatty acid transport by fatty acid translocase/CD36. Proc. Nutr. Soc., **63**, 245-249.

Dennis, G. Jr., Sherman, B.T., Hosack, D.A., Yang, J., Gao, W., Lane, H.C. and Lempicki, R.A. (2003): DAVID: Database for annotation, visualization, and integrated discovery. Genome Biol., **4**, 3.

De Sandro, V., Chevrier, M., Boddaert, A., Melcion, C., Cordier, A. and Richert, L. (1991): Comparison of the effects of propylthiouracil, amiodarone, diphenylhydantoin, phenobarbital, and 3-methylcholanthrene on hepatic and renal T4 metabolism and thyroid gland function in rats. Toxicol. Appl. Pharmacol., **111**, 263-278.

Diekman, M.J., Anghelescu, N., Endert, E., Bakker, O. and Wiersinga, W.M. (2000): Changes in plasma low-density lipoprotein (LDL)- and high-density lipoprotein cholesterol in hypo- and hyperthyroid patients are related to changes in free thyroxine, not to polymorphisms in LDL

receptor or cholesterol ester transfer protein genes. J. Clin. Endocrinol. Metab., **85**, 1857-1862.

Goudriaan, J.R., den Boer, M.A., Rensen, P.C., Febbraio, M., Kuipers, F., Romijn, J.A., Havekes, L.M. and Voshol, P.J. (2005): CD36 deficiency in mice impairs lipoprotein lipase-mediated triglyceride clearance. J. Lipid Res., **46**, 2175-2181.

Gullberg, H., Rudling, M., Forrest, D., Angelin, B. and Vennstrom, B. (2000): Thyroid hormone receptor beta-deficient mice show complete loss of the normal cholesterol 7alpha-hydroxylase (CYP7A) response to thyroid hormone but display enhanced resistance to dietary cholesterol. Mol. Endocrinol., **14**, 1739-1749.

Gullberg, H., Rudling, M., Salto, C., Forrest, D., Angelin, B. and Vennstrom, B. (2002): Requirement for thyroid hormone receptor beta in T3 regulation of cholesterol metabolism in mice. Mol. Endocrinol., **16**, 1767-1777.

Hall, I.H., Patrick, M.A. and Maguire, J.H. (1990): Hypolipidemic activity in rodents of phenobarbital and related derivatives. Arch. Pharmacol., **323**, 579-586.

Hashimoto, K., Cohen, R.N., Yamada, M., Markan, K.R., Monden, T., Satoh, T., Mori, M. and Wondisford, F.E. (2006): Cross-talk between thyroid hormone receptor and liver X receptor regulatory pathways is revealed in a thyroid hormone resistance mouse model. J. Biol. Chem., **281**, 295-302.

Hibbs, K., Skubitz, K.M., Pambuccian, S.E., Casey, R.C., Burleson, K.M., Oegema, Jr. T.R., Thiele, J.J., Grindle, S.M., Bliss, R.L. and Skubitz, A.P.N. (2004): Differential gene expression in ovarian carcinoma. Identification of potential biomarkers. Am. J. Pathol., **165**, 397-414.

Kakizaki, S., Yamamoto, Y., Ueda, A., Moore, R., Sueyoshi, T. and Negishi, M. (2003): Phenobarbital induction of drug/steroid-metabolizing enzymes and nuclear receptor CAR. Biochim. Biophys. Acta, **1619**, 239-242.

Kern, P.A., Ranganathan, G., Yukht, A., Ong, J.M. and Davis, R.C. (1996): Translational regulation of lipoprotein lipase by thyroid hormone is via a cytoplasmic repressor that interacts with the 3' untranslated region. J. Lipid Res., **37**, 2332-2340.

Kersten, S., Seydoux, J., Peters, J.M., Gonzalez, F.J., Desvergne, B. and Wahli, W. (1999): Peroxisome proliferator-activated receptor alpha mediates the adaptive response to fasting. J. Clin. Invest., **103**, 1489-1498.

Kiyosawa, N., Tanaka, K., Hirao, J., Ito, K., Niino, N., Sakuma, K., Kanbori, M., Yamoto, T., Manabe, S. and Matsunuma, N. (2004): Molecular mechanism investigation of phenobarbital-induced serum cholesterol elevation in rat livers by microarray analysis. Arch. Toxicol., **78**, 435-442.

Kunishima, C., Inoue, I., Oikawa, T. and Katayama, S. (2003): The metabolism, toxicity and pharmacological studies of benzbromarone (Urinorm®). J. Saitama Med. School, **30**, 187-194.

Lee, S.S., Chan, W.Y., Lo, C.K., Wan, D.C., Tsang, D.S. and Cheung, W.T. (2004): Requirement of PPARalpha in maintaining phospholipid and triacylglycerol homeostasis during energy deprivation. J. Lipid Res., **45**, 2025-2037.

Leone, T.C., Weinheimer, C.J. and Kelly, D.P. (1999): A critical role for the peroxisome proliferator-activated receptor alpha (PPARalpha) in the cellular fasting response: The PPARalpha-null mouse as a model of fatty acid oxidation disorders. Proc. Nat. Acad. Sci. USA, **96**, 7473-7478.

Maglich, J.M., Watson, J., McMillen, P.J., Goodwin, B., Willson, T.M. and Moore, J.T. (2004): The nuclear receptor CAR is a regulator of thyroid hormone metabolism during caloric restriction. J. Biol. Chem., **279**, 19832-19838.

Masubuchi, N., Hakusui, H. and Okazaki, O. (1997): Effects of proton pump inhibitors on thyroid hormone metabolism in rats: A comparison of UDP-glucuronyltransferase induction. Biochem. Pharmacol., **54**, 1225-1231.

McCarthy, T.C., Pollak, P.T., Hanniman, E.A. and Sinal, C.J. (2004): Disruption of hepatic lipid homeostasis in mice after amiodarone treatment is associated with peroxisome proliferator-activated receptor-alpha target gene activation. J. Pharm. Exp. Ther., **311**, 864-873.

Motojima, K., Passilly, P., Peters, J.M., Gonzalez, F.J. and Latruffe, N. (1998): Expression of putative fatty acid transporter genes are regulated by peroxisome proliferator-activated receptor alpha and gamma activators in a tissue- and inducer-specific manner. J. Biol. Chem., **273**, 16710-16714.

Mutlib, A., Joang, P., Antherton, J., Obert, L., Kostrubsky, S., Madore, S. and Nelson, S. (2006): Identifiation of potential genomic biom-

arkers of hepatotoxicity caused by reactive metabolites of *N*-methylformamide: Application of stable isotope labeled compounds in toxicogenomic studies. Chem. Res. Toxicol., **19**, 1270-1283.

Ness, G.C. and Chambers, C.M. (2000): Feedback and hormonal regulation of hepatic 3-hydroxy-3-methylglutaryl coenzyme A reductase: The concept of cholesterol buffering capacity. Proc. Soc. Exp. Biol. Med., **224**, 8-19.

Ong, J.M., Simsolo, R.B., Saghizadeh, M., Pauer, A. and Kern, P.A. (1994): Expression of lipoprotein lipase in rat muscle: Regulation by feeding and hypothyroidism. J. Lipid Res., **35**, 1542-1551.

Pitari, G., Malergue, F., Martin, F., Philippe, J.M., Massucci, M.T., Chabret, C., Maras, B., Dupre, S., Naquet, P. and Galland, F. (2000): Pantetheinase activity of membrane-bound Vanin-1: Lack of free cysteamine in tissues of Vanin-1 deficient mice. FEBS Lett., **483**, 149-154.

Qatanani, M. and Moore, D.D. (2005): CAR, the continuously advancing receptor, in drug metabolism and disease. Curr. Drug Metab., **6**, 329-339.

Schoonjans, K., Staels, B. and Auwerx, J. (1996): Role of the peroxisome proliferator-activated receptor (PPAR) in mediating the effects of fibrates and fatty acids on gene expression. J. Lipid Res., **37**, 907-925.

Snedecor, G.W. and Cochran, W.G. (1989): Statistical Methods, 8th ed., Iowa State University Press.

Staels, B., Vu-Dac, N., Kosykh, V.A., Saladin, R., Fruchart, J.C., Dallongeville, J. and Auwerx, J. (1995): Fibrates downregulate apolipoprotein C-III expression independent of induction of peroxisomal acyl coenzyme A oxidase. A potential mechanism for the hypolipidemic action of fibrates. J. Clin. Invest., **95**, 705-712.

Tan, Y., Shi, L., Hussain, S.M., Xu, J., Tong, W., Frazier, J.M. and Wang, C. (2006): Integrating time-course microarray gene expression profiles with cytotoxicity for identification of biomarkers in primary rat hepatocytes exposed to cadmium. Bioinformatics, **22**, 77-87.

Urushidani, T. and Nagao, T. (2005): Toxicogenomics: The Japanese initiative. In (Borlak, J., ed.), Handbook of Toxicogenomics - Strategies and Applications, Wiley - VCH, pp. 623-631.

van Raalte, D.H., Li, M., Pritchard, P.H. and Wasan, K.M. (2004): Peroxisome proliferator-activated receptor (PPAR)-alpha: A pharmacological target with a promising future. Pharmaceut. Res., **21**, 1531-1538.

Weiss, R.E., Murata, Y., Cua, K., Hayashi, Y., Seo, H. and Refetoff, S. (1998): Thyroid hormone action on liver, heart, and energy expenditure in thyroid hormone receptor beta-deficient mice. Endocrinol., **139**, 4945-4952.

Yamazaki, K., Kuromitsu, J. and Tanaka, I. (2002): Microarray analysis of gene expression changes in mouse liver induced by peroxisome proliferator- activated receptor alpha agonists. Biochem. Biophys. Res. Comm., **290**, 1114-1122.

Zhou, Z., Yon, T.-S., Chen, Z., Guo, K., Ng, C.P., Ponniah, S., Lin, S.C., Hong, W. and Li, P. (2003): Cidea-deficient mice have lean phenotype and are resistant to obesity. Nat. Genet., **35**, 49-56.

The Journal of Toxicological Sciences,
Vol.32, No.5, 469-486, 2007

IDENTIFICATION OF GLUTATHIONE DEPLETION-RESPONSIVE GENES USING PHORONE-TREATED RAT LIVER

Naoki KIYOSAWA[1], Takeki UEHARA[1], Weihua GAO[1], Ko OMURA[1], Mitsuhiro HIRODE[1], Toshinobu SHIMIZU[1], Yumiko MIZUKAWA[1,2], Atsushi ONO[1], Toshikazu MIYAGISHIMA[1], Taku NAGAO[3] and Tetsuro URUSHIDANI[1,2]

[1]*Toxicogenomics Project, National Institute of Biomedical Innovation, 7-6-8 Asagi, Ibaraki, Osaka 567-0085, Japan*

[2]*Department of Pathophysiology, Faculty of Pharmaceutical Sciences, Doshisha Women's College of Liberal Arts, Kodo, Kyotanabe, Kyoto 610-0395, Japan*

[3]*National Institute of Health Sciences, 1-18-1 Kamiyoga, Setagaya-Ku, Tokyo 158-8501, Japan*

(Received August 17, 2007; Accepted August 27, 2007)

ABSTRACT — To identify candidate biomarker gene sets to evaluate the potential risk of chemical-induced glutathione depletion in livers, we conducted microarray analysis on rat livers administered with phorone (40, 120 and 400 mg/kg), a prototypical glutathione depletor. Hepatic glutathione content was measured and glutathione depletion-responsive gene probe sets (GSH probe sets) were identified using Affymetrix Rat Genome 230 2.0 GeneChip by the following procedure. First, probe sets, whose signal values were inversely correlated with hepatic glutathione content throughout the experimental period, were statistically identified. Next, probe sets, whose average signal values were greater than 1.5-fold compared to those of controls 3 hr after phorone treatment, were selected. Finally, probe sets without unique Entrez Gene ID were removed, ending up with 161 probe sets in total. The usefulness of the identified GSH probe sets was verified by a toxicogenomics database. It was shown that signal profiles of the GSH probe sets in rats treated with bromobenzene were strongly altered compared with other chemicals. Focusing on bromobenzene, time-course profiles of hepatic glutathione content and gene expression revealed that the change in gene expression profile was marked after the bromobenzene treatment, whereas hepatic glutathione content had recovered after initial acute depletion, suggesting that the gene expression profile did not reflect the hepatic glutathione content itself, but rather reflects a perturbation of glutathione homeostasis. The identified GSH probe sets would be useful for detecting glutathione-depleting risk of chemicals from microarray data.

KEY WORDS: Glutathione, Rat, Liver, Microarray, Toxicity, Toxicogenomics, Phorone

INTRODUCTION

Microarray analysis displays tens of thousands of nucleotide probes on a substrate surface, and enables the measurement of mRNA levels of large numbers of genes simultaneously (Rockett and Dix, 2000). Microarray analysis is aimed at toxicological investigation and is called toxicogenomics (Boverhof and Zacharewski, 2006). This is thought to be useful for such points as: I) understanding the molecular mechanisms of toxicity, II) the early prediction of drug toxicity risk, and III) improvement in extrapolation of experimental animal data to humans (Orphanides, 2003). At present, the liver is one of the most favored target organs in Toxicogenomics studies for the following reasons: 1) it is exposed to relatively higher levels of administered drugs, 2) it is a relatively homogenous organ and thus easy to sample, and 3) it can dramatically affect the pharmaco/toxico-kinetics of the drugs in the body by the first-pass effect (Parkinson, 2001). Furthermore, hepatotoxicity has been a critical concern in drug development (Kaplowitz, 2004; Li, 2002).

Correspondence: Tetsuro URUSHIDANI (E-mail: turushid@dwc.doshisha.ac.jp)

These issues have motivated toxicologists to investigate liver toxicity using the toxicogenomics technique.

The Toxicogenomics Project in Japan (TGP; http://wwwtgp.nibio.go.jp/index-e.html) has been completed by the National Institute of Health Sciences and 17 pharmaceutical companies after 5 years' collaboration from 2002 (Urushidani and Nagao, 2005; Takashima *et al.*, 2006). In the project, five rats per group were administered with toxicological prototype drugs once daily, where three dose-ranges were set, and liver samples were collected 3, 6, 9 and 24 hr after a single treatment, as well as 4, 9, 15 and 29 days after repetitive treatment. Of the collected liver samples, three samples per group were subjected to microarray analysis using the Affymetrix GeneChip system. In addition, toxicological data, such as blood chemistry and histopathology, were collected simultaneously. Such a large-scale database would be invaluable for scientists not only as a reference database but also as a resource for screening candidate toxicogenomic biomarker sets.

Glutathione serves vital functions in detoxifying electrophiles and scavenging free radicals (Lu, 1999), and hepatotoxicity caused by glutathione depletion has been intensely investigated. In the case of acetaminophen overdosage, acetaminophen is metabolically activated by phase I drug metabolizing enzymes to form a reactive metabolite, *N*-acetyl-*p*-benzoquinone imine (NAPQI), which covalently binds to proteins (Dahlin *et al.*, 1984; James *et al.*, 2003). Although NAPQI can be detoxified by glutathione conjugation under ordinary conditions, an excess dose of acetaminophen depletes 90% of hepatic glutathione, and reactive NAPQI forms protein adducts (Mitchell *et al.*, 1973; James *et al.*, 2003), resulting in hepatocyte necrosis.

Previously, sixty-nine gene probe sets of Rat Genome U34A GeneChip (Affymetrix, Inc.) were identified as glutathione depletion-responsive genes, using L-buthionine-(S,R)-sulfoximine (BSO) as a glutathione-depleting agent (Kiyosawa *et al.*, 2004). Although the probe sets were thought to be useful for evaluation of drug-induced glutathione deficiency in rat liver, the study had two major drawbacks. First, the sample size used for the study was relatively small: one dose setting and one time point of observation, using 4 rats per group. Secondly, BSO depletes hepatic glutathione by inhibiting γ-glutamylcysteine synthetase, a key enzyme of glutathione synthesis (Moinova and Mulcahy, 1999). In the case of acetaminophen-induced glutathione depletion, an overdose of acetaminophen depletes hepatic glutathione by extended conjugation of glutathione with activated metabolites such as NAPQI. Therefore, BSO-induced glutathione depletion would probably not appropriately reflect the drug-induced one. For these reasons, an alternative glutathione-depleting model, other than the BSO model, would be useful for better explaining drug-induced glutathione depletion, in view of the gene expression profile.

Phorone is an α, β-unsaturated compound, which strongly depletes hepatic glutathione content by conjugation with glutathione, by action of glutathione *S*-transferase (GST), and is excreted from liver (Boyland and Chasseaud, 1967; van Doorn *et al.*, 1978). Comparing the glutathione-depleting mechanism of phorone with that of BSO, the phorone-induced glutathione depletion mechanism is thought to be more similar to that induced by acetaminophen overdosing, where activated metabolites such as NAPQI deplete glutathione by being conjugated with glutathione and then are excreted from liver.

In this paper, we present candidate biomarker probe sets of RAE 230A GeneChip for evaluation of the potential risk of drug-induced glutathione depletion in rat livers, using phorone as a glutathione-depleting agent. The toxicological significance of identified biomarker probe sets was examined using a large-scale TGP database.

MATERIALS AND METHODS

Chemicals

Phorone, acetaminophen, thioacetamide, phenylbutazone, glibenclamide, methapyrilene hydrochloride and perhexiline maleate were purchased from Sigma-Aldrich (St. Louis, MO, USA). Clofibrate, aspirin and chlorpromazine were purchased from Wako Pure Chemical Industries (Osaka, Japan). Bromobenzene, hexachlorobenzene, carbon tetrachloride and coumarin were purchased from Tokyo Chemical Industry (Tokyo, Japan).

Animal treatment

Six-week old-male Crj:CD(SD)IGS rats (Charles River Japan, Kanagawa, Japan) were used in the study. The animals were individually housed in stainless-steel cages in a room that was lighted for 12 hr (7:00-19:00) daily, ventilated with an air-exchange rate of 15 times per hour, and maintained at 21-25°C with a relative humidity of 40-70%. Each animal was allowed free access to water and pellet food (CRF-1, sterilized by

radiation, Oriental Yeast Co., Japan). Five rats per group were administered with phorone (40, 120 or 400 mg/kg, i.p.). Five rats per group were administered orally with acetaminophen (1000 mg/kg), bromobenzene (300 mg/kg), clofibrate (300 mg/kg), chlorpromazine (45 mg/kg), glibenclamide (1000 mg/kg), methapyrilene (100 mg/kg), phenylbutazone (200 mg/kg), aspirin (450 mg/kg), carbon tetrachloride (300 mg/kg), coumarin (150 mg/kg), hexachlorobenzene (300 mg/kg), perhexiline maleate (150 mg/kg) or thioacetamide (45 mg/kg). Blood samples were collected in tubes containing heparin lithium 3, 6, 9, or 24 hr after treatment for biochemical assay. The animals were then euthanized and the liver was removed and soaked in RNA*later* (Ambion, Austin, TX, USA) immediately after sampling and stored at −80°C until use for gene expression analysis. In the animals treated with phorone or bromobenzene, another aliquot of liver sample was immediately frozen in liquid nitrogen for measurement of hepatic glutathione contents. The remaining liver samples were then removed and fixed in 10% neutral buffered formalin for histopathological examination. The experimental protocol was reviewed and approved by the Ethics Review Committee for Animal Experimentation of the National Institute of Health Sciences.

Plasma biochemistry

Activities of alanine aminotransferase (ALT) and aspartate aminotransferase (AST) in plasma were determined using a 7080 Clinical Analyzer (Hitachi High-Technologies Corporation, Tokyo, Japan).

Histopathology

The fixed samples were dehydrated through graded alcohols and embedded in paraffin. Serial sections 2-3 μm thick were stained with hematoxylin and eosin for pathological examination.

Measurement of hepatic glutathione content

The liver samples (0.1 g) were homogenized with 5% 5-sulfosalicylic acid (Sigma-Aldrich) and centrifuged at 12,000 rpm for 10 min at 4°C. The supernatant was used for the measurement of total glutathione content in the liver using theTotal Glutathione Quantification Kit (Dojindo Laboratories), according to the manufacturer's instructions.

Microarray analysis

Liver samples were homogenized with RLT buffer, supplied in the RNeasy Mini Kit (Qiagen, Valencia, CA, USA), using Mill Mixer (Qiagen) and zirconium beads. Total RNA was isolated using Bio Robot 3000 (Qiagen). DNase I treatment was performed using RNase-Free DNase set (Qiagen) for 15 min at room temperature. GeneChip analysis was performed on 3 out of 5 samples in each group according to the Affymetrix standard protocol. Briefly, a total of RNA of 5 μg prepared from the individual rat liver samples was used for cDNA synthesis using the T7-$(dT)_{24}$ primer (Affymetrix) and Superscript Choice System (Invitrogen, Carlsbad, CA, USA). The cDNA was purified using cDNA Cleanup Module (Affymetrix), and biotin-labeled cRNA mix was transcribed using the BioArray High Yield RNA Transcription Labeling Kit (Enzo Diagnostics, Farmingdale, NY, USA). Ten micrograms of fragmented cRNA cocktails were hybridized to the RAE 230A GeneChip array for all samples except for that of phorone- and corresponding vehicle-treated rats, which were hybridized to the RAE 230 2.0 array for 18 hr at 45°C at 60 rpm. GeneChip was washed and stained using Fluidics Station 400 (Affymetrix) according to the Affymetrix standard protocol and scanned using Gene Array Scanner (Affymetrix). The scanned data images were digitalized using Affymetrix Microarray Suite ver. 5.0 (Affymetrix), and the data was scaled by adjusting the mean Signal value to 500.

Microarray data analysis

We primarily use gloval mean normalization for data analysis in our project. Firstly, using vehicle- and phorone (40 and 120 mg/kg)-treated rats, where the total number of rats was 36, both Spearman's and Pearson's correlation coefficients between the signal value and hepatic glutathione content were calculated for all the probe sets that existed on the RAE 230A array. The probe sets with both Spearman's coefficients and Pearson's coefficients less than -0.329 were chosen as statistically significant inverse correlations ($N=36, p < 0.05$). Secondly, probe sets, whose average signal values in 120 mg/kg phorone-treated rats at 3 h were above 1.5 compared to those of corresponding controls were selected. Then, probe sets, whose detection calls determined by Microarray Suite ver. 5.0 were all present 3 hr after phorone treatment, were selected. Finally, annotation for each probe set was obtained using NetAffx Website (Liu *et al.*, 2003), and probe sets without unique Entrez Gene ID were excluded from the analysis. For each probe set, the signal data was z-score normalized in the vehicle- and phorone (40, 120 and 400 mg/kg)-treated group. All the z-score

normalized signal data were presented as a heat map and z-score normalized glutathione content data was also presented as a heat map.

Statistical analysis

Dunnett's test was performed for serum chemistry and glutathione content data (between phorone-treated rat groups and vehicle-treated group at the same time point), using R software (www.r-project.org). Serum chemistry data (other than that of phorone-treated rats) was analyzed by F-test to evaluate the homogeneity of variance. If the variance was homogeneous, Student's *t*-test was applied. If the variance was heterogeneous, Aspin-Welch's *t*-test was performed (Snedecor and Cochran, 1989). F-test, Student's *t*-test and Aspin-Welch's *t*-test were performed using Microsoft Excel 2007. Both Spearman's and Pearson's correlation coefficients were calculated using Microsoft Excel 2007. A p-value of < 0.05 was considered statistically significant. Principal component analysis (PCA) was performed using the Spotfire Functional Genomics Package ver. 17.4.832 (Spotfire, Somerville, MA, USA).

RESULTS

Plasma biochemistry in phorone-treated rats

There were no apparent fluctuations of plasma ALT activity in 40 and 120 mg/kg phorone-treated rats throughout the experimental period (Fig. 1). Plasma ALT activity was obviously elevated in rats 24 hr after 400 mg/kg phorone treatment.

Glutathione content in phorone-treated rat liver

Hepatic glutathione content was significantly decreased 3, 6 and 9 hr for 40 mg/kg phorone-treated rats, and recovered above the control level 24 hr after treatment (Fig. 2). Hepatic glutathione content was significantly decreased to an 8.3-fold lower level compared with the control 3 hr after the 120 mg/kg phorone-treated rats, and gradually recovered 6 and 9 hr after treatment, resulting in a 1.52-fold higher level compared with control 24 hr after treatment. Hepatic glutathione content was significantly decreased to a 22- to 30-fold lower level compared with control 3, 6 and 9 hr after the 400 mg/kg phorone-treated rats, and recovered to the control level 24 hr after treatment.

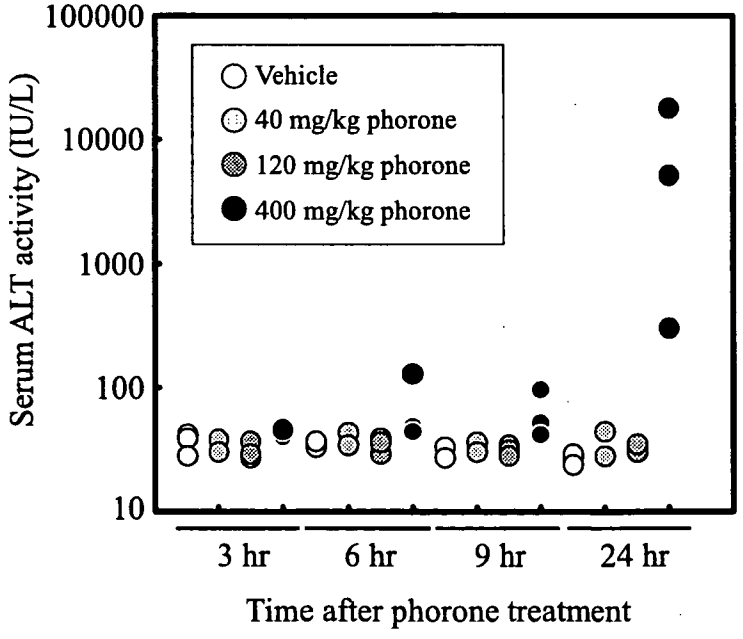

Fig. 1. Activity of alanine aminotransferase in plasma. Each dot represents the value of an individual animal.

Identification of glutathione deficiency-correlated gene probe sets

A hundred and sixty-one probe sets were identified as glutathione deficiency-correlated gene probe sets, or GSH probe sets (Table 1), and classified to 5 groups, i.e., "antioxidant, phase II drug metabolizing enzymes, and oxidative stress markers" (11 probe sets), "transporter" (13 probe sets), "metabolism" (20 probe sets), "transcription factors and signal transduction-related, and protein turnover-related genes" (79 probe sets), and "miscellaneous" (37 probe sets). Both the z-score transformed hepatic glutathione content and z-score transformed signal levels of the GSH probe sets are presented as a heat map (Fig. 3). PCR primers and TaqMan probes for 4 genes from the list above, namely tribbles homolog 3 (accession no. AB020967), heme oxygenase-1 (NM_012580), thioredoxin reductase-1 (NM_031614) and γ-glutamylcysteine synthetase modifier subunit (NM_017305), were synthesized and quantitative RT-PCR was performed using the TaqMan Universal PCR Master Mix (Applied Biosystems), and the mRNA level was quantified with a GeneAmp 5700 Sequence Detection System (Applied Biosystems) according to the manufacturer's instructions. It was confirmed that quantification by GeneChip was sufficient (data not shown).

Plasma biochemistry and histopathological findings in rat liver treated with various hepatotoxicants

Rats treated with bromobenzene, methapyrilene or thioacetamide showed significant increase in plasma ALT activity 24 hr after treatment (Table 2). Rats treated with acetaminophen, chlorpromazine, glibenclamide or methapyrilene showed significant increase in serum AST activity 24 hr after treatment. Rats treated with acetaminophen, bromobenzene, methapyrilene, carbon tetrachloride, coumarin or thioacetamide showed histopathological changes 24 hr after treatment, while rats treated with clofibrate, chlorpromazine, glibenclamide, phenylbutazone, aspirin,

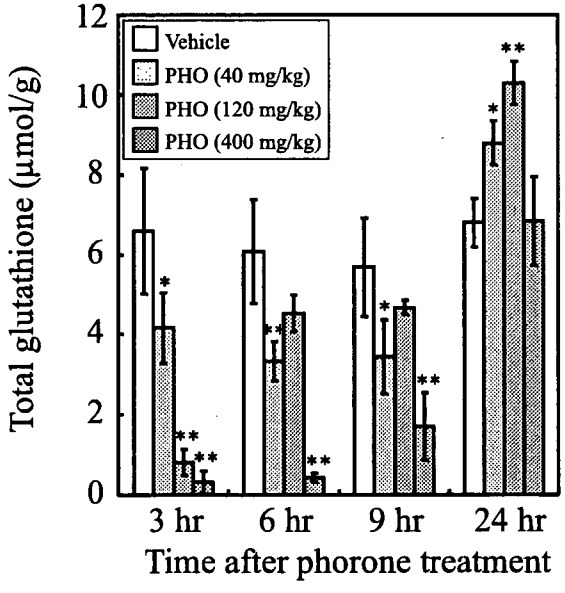

Fig. 2. Hepatic glutathione content after phorone treatment.
Three rats per group were treated with 40, 120 or 400 mg/kg phorone or vehicle, and the livers were removed 3, 6, 9 and 24 hr after treatment. Hepatic glutathione content (total) was measured and the data are presented as mean ± S.D. ** and *, $p<0.01$ and $p<0.05$ by Dunnett's test, respectively.

Table 1. Glutathione depletion-responsive gene probe sets (GSH probe sets).

Affymetrix probe ID	Correlation coefficient		Gene Symbol	Annotation
	Spearman's	Pearson's		
Antioxidant, phase II drug-metabolizing enzymes and oxidative stress markers				
1368037_at	−0.602	−0.368	Cbr1	carbonyl reductase 1
1387221_at	−0.720	−0.712	Gch	GTP cyclohydrolase 1
1368503_at	−0.702	−0.650	Gch	GTP cyclohydrolase 1
1370030_at	−0.570	−0.448	Gclm	glutamate cysteine ligase, modifier subunit
1370080_at	−0.611	−0.609	Hmox1	heme oxygenase (decycling) 1
1387282_at	−0.680	−0.589	Hspb8	heat shock 22kDa protein 8
1388721_at	−0.747	−0.660	Hspb8	heat shock 22kDa protein 8
1389578_at	−0.649	−0.582	Isrip	ischemia/reperfusion inducible protein
1372510_at	−0.589	−0.578	Srxn1	Sulfiredoxin 1 homolog (S. cerevisiae)
1398791_at	−0.600	−0.471	Txnrd1	thioredoxin reductase 1
1386958_at	−0.666	−0.459	Txnrd1	thioredoxin reductase 1
Transporter				
1374423_at	−0.711	−0.688	Hiat1_predicted	hippocampus abundant gene transcript 1 (predicted)
1370934_at	−0.656	−0.579	Nup153	nucleoporin 153
1367803_at	−0.430	−0.523	Nup54	nucleoporin 54
1371754_at	−0.330	−0.497	Slc25a25	solute carrier family 25 (mitochondrial carrier, phosphate carrier), member 25
1369099_at	−0.356	−0.567	Slc30a1	solute carrier family 30 (zinc transporter), member 1
1370286_at	−0.858	−0.813	Slc38a2	solute carrier family 38, member 2
1398771_at	−0.651	−0.520	Slc3a2	solute carrier family 3 (activators of dibasic and neutral amino acid transport), member 2
1387130_at	−0.726	−0.455	Slc40a1	solute carrier family 39 (iron-regulated transporter), member 1
1387693_a_at	−0.731	−0.601	Slc6a9	solute carrier family 6 (neurotransmitter transporter, glycine), member 9
1369772_at	−0.609	−0.473	Slc6a9	solute carrier family 6 (neurotransmitter transporter, glycine), member 9
1373787_at	−0.619	−0.513	Slc6a9	solute carrier family 6 (neurotransmitter transporter, glycine), member 9
1368391_at	−0.780	−0.700	Slc7a1	solute carrier family 7 (cationic amino acid transporter, y^+ system), member 1
1368392_at	−0.591	−0.626	Slc7a1	solute carrier family 7 (cationic amino acid transporter, y^+ system), member 1
Metabolism				
1387925_at	−0.747	−0.574	Asns	asparagine synthetase
1386928_at	−0.352	−0.409	Bcat2	branched chain aminotransferase 2, mitochondrial
1374034_at	−0.762	−0.756	Cars_predicted	cysteinyl-tRNA synthetase (predicted)
1368709_at	−0.537	−0.492	Fut1	fucosyltransferase 1
1375852_at	−0.441	−0.532	Hmgcr	3-hydroxy-3-methylglutaryl-Coenzyme A reductase
1387848_at	−0.413	−0.500	Hmgcr	3-hydroxy-3-methylglutaryl-Coenzyme A reductase
1376418_a_at	−0.679	−0.549	Iars_predicted	isoleucine-tRNA synthetase (predicted)

Table 1. Continued.

Affymetrix probe ID	Correlation coefficient		Gene Symbol	Annotation
	Spearman's	Pearson's		
1389551_at	−0.373	−0.359	Lactb2	lactamase, beta 2
1371350_at	−0.773	−0.683	LOC683283	similar to S-adenosylmethionine synthetase isoform type-2 (Methionine adenosyltransferase 2) (AdoMet synthetase 2) (Methionine adenosyltransferase II) (MAT-II)
1377287_at	−0.495	−0.532	Mars2_predicted	methionine-tRNA synthetase 2 (mitochondrial) (predicted)
1375684_at	−0.554	−0.490	Neu1	neuraminidase 1
1367811_at	−0.675	−0.459	Phgdh	3-phosphoglycerate dehydrogenase
1369785_at	−0.754	−0.691	Ppat	phosphoribosyl pyrophosphate amidotransferase
1388756_at	−0.614	−0.529	Ppcs	phosphopantothenoylcysteine synthetase
1372665_at	−0.682	−0.633	Psat1	phosphoserine aminotransferase 1
1375964_at	−0.641	−0.615	Psph	phosphoserine phosphatase
1388521_at	−0.428	−0.544	Pycs_predicted	pyrroline-5-carboxylate synthetase (glutamate gamma-semialdehyde synthetase) (predicted)
1372602_at	−0.490	−0.460	RGD1311800	similar to genethonin 1
1398452_at	−0.421	−0.431	RGD1559923_predicted	similar to chromosome 14 open reading frame 35 (predicted)
1372009_at	−0.569	−0.478	Yars	tyrosyl-tRNA synthetase
Transcription factor, signal transduction-related and protein turnover-related gene				
1388179_at	−0.370	−0.379	Acvr2b	activin receptor IIB
1369146_a_at	−0.433	−0.479	Ahr	aryl hydrocarbon receptor
1378140_at	−0.600	−0.606	Arl11	ADP-ribosylation factor-like 11
1367960_at	−0.470	−0.485	Arl4a	ADP-ribosylation factor-like 4A
1389623_at	−0.605	−0.623	Atf1	activating transcription factor 1
1375941_at	−0.594	−0.513	Baiap2l1	BAI1-associated protein 2-like 1
1374947_at	−0.584	−0.567	Bcar3_predicted	breast cancer anti-estrogen resistance 3 (predicted)
1376754_at	−0.771	−0.740	Cars_predicted	cysteinyl-tRNA synthetase (predicted)
1391572_at	−0.804	−0.802	Cars_predicted	cysteinyl-tRNA synthetase (predicted)
1387087_at	−0.720	−0.734	Cebpb	CCAAT/enhancer binding protein (C/EBP), beta
1387244_at	−0.504	−0.371	Cgrrf1	cell growth regulator with ring finger domain 1
1372498_at	−0.626	−0.608	Ciapin1	cytokine induced apoptosis inhibitor 1
1399141_at	−0.640	−0.664	Clk4	CDC like kinase 4
1376811_a_at	−0.571	−0.534	Cpsf6_predicted	cleavage and polyadenylation specific factor 6, 68kDa (predicted)
1369737_at	−0.558	−0.614	Crem	cAMP responsive element modulator
1370979_at	−0.433	−0.475	Ddx20	DEAD/H (Asp-Glu-Ala-Asp/His) box polypeptide 20, 103kD
1375901_at	−0.497	−0.360	Ddx21a	DEAD (Asp-Glu-Ala-Asp) box polypeptide 21a
1373200_at	−0.581	−0.505	Eef1e1_predicted	eukaryotic translation elongation factor 1 epsilon 1 (predicted)

Table 1. Continued.

Affymetrix probe ID	Correlation coefficient		Gene Symbol	Annotation
	Spearman's	Pearson's		
1368967_at	−0.629	−0.484	Eif2b3	eukaryotic translation initiation factor 2B, subunit 3 gamma
1386888_at	−0.794	−0.776	Eif4ebp1	eukaryotic translation initiation factor 4E binding protein 1
1388666_at	−0.581	−0.588	Encl	ectodermal-neural cortex 1
1382059_at	−0.593	−0.634	Fbxo30	F-box protein 30
1372526_at	−0.675	−0.776	Flcn	folliculin
1374530_at	−0.671	−0.601	Fzd7_predicted	frizzled homolog 7 (Drosophila) (predicted)
1373499_at	−0.731	−0.622	Gas5	growth arrest specific 5
1388953_at	−0.682	−0.665	Gnl3	guanine nucleotide binding protein-like 3 (nucleolar)
1373094_at	−0.788	−0.587	Gtf2h1_predicted	general transcription factor II H, polypeptide 1 (predicted)
1367741_at	−0.618	−0.579	Herpud1	homocysteine-inducible, endoplasmic reticulum stress-inducible, ubiquitin-like domain member 1
1372693_at	−0.462	−0.559	Hnrpa1	heterogeneous nuclear ribonucleoprotein A1
1387430_at	−0.754	−0.774	Hsf2	heat shock factor 2
1388587_at	−0.571	−0.636	Ier3	immediate early response 3
1367795_at	−0.666	−0.597	Ifrd1	interferon-related developmental regulator 1
1368160_at	−0.644	−0.700	Igfbp1	insulin-like growth factor binding protein 1
1387440_at	−0.432	−0.330	Ireb2	iron responsive element binding protein 2
1373374_at	−0.813	−0.812	Lmo4	LIM domain only 4
1373303_at	−0.339	−0.409	LOC312030	similar to splicing factor, arginine/serine-rich 2, interacting protein
1374154_at	−0.762	−0.677	LOC312030	Similar to splicing factor, arginine/serine-rich 2, interacting protein
1374857_at	−0.555	−0.445	LOC499709	similar to nucleolar protein family A, member 1
1373133_at	−0.630	−0.692	LOC500282	similar to ADP-ribosylation factor-like 10C
1368874_a_at	−0.775	−0.801	Mafg	v-maf musculoaponeurotic fibrosarcoma oncogene family, protein G (avian)
1368273_at	−0.342	−0.453	Mapk6	mitogen-activated protein kinase 6
1384427_at	−0.766	−0.764	Mdm2_predicted	transformed mouse 3T3 cell double minute 2 homolog (mouse) (predicted)
1388990_at	−0.544	−0.492	Mki67ip	Mki67 (FHA domain) interacting nucleolar phosphoprotein
1375442_at	−0.670	−0.696	Mphosph10_predicted	M-phase phosphoprotein 10 (U3 small nucleolar ribonucleoprotein) (predicted)
1368308_at	−0.513	−0.622	Myc	myelocytomatosis viral oncogene homolog (avian)
1374437_at	−0.717	−0.665	Nars	asparaginyl-tRNA synthetase
1376704_a_at	−0.577	−0.485	Ndnl2	necdin-like 2
1389996_at	−0.645	−0.657	Nek1_predicted	NIMA (never in mitosis gene a)-related expressed kinase 1 (predicted)
1389765_at	−0.564	−0.579	Nle1_predicted	notchless homolog 1 (Drosophila) (predicted)
1368173_at	−0.444	−0.403	Nol5	nucleolar protein 5
1368032_at	−0.451	−0.365	Nolc1	nucleolar and coiled-body phosphoprotein 1
1387152_at	−0.375	−0.508	Nrbf2	nuclear receptor binding factor 2

Table 1. Continued.

Affymetrix probe ID	Correlation coefficient		Gene Symbol	Annotation
	Spearman's	Pearson's		
1368068_a_at	−0.605	−0.488	Pacsin2	protein kinase C and casein kinase substrate in neurons 2
1372857_at	−0.720	−0.706	Pacsin2	protein kinase C and casein kinase substrate in neurons 2
1374326_at	−0.576	−0.544	Ppan	peter pan homolog (Drosophila)
1369104_at	−0.618	−0.554	Prkaa1	protein kinase, AMP-activated, alpha 1 catalytic subunit
1368087_a_at	−0.419	−0.407	Ptpn21	protein tyrosine phosphatase, non-receptor type 21
1371081_at	−0.740	−0.765	Rapgef4	Rap guanine nucleotide exchange factor (GEF) 4
1374750_at	−0.773	−0.799	Rapgef6_predicted	Rap guanine nucleotide exchange factor (GEF) 6 (predicted)
1388522_at	−0.689	−0.713	RGD1310383_predicted	similar to T-cell activation protein phosphatase 2C (predicted)
1374945_at	−0.587	−0.463	RGD1359191	GCD14/PCMT domain containing protein RGD1359191
1373075_at	−0.762	−0.664	RGD1560888_predicted	similar to Cell division protein kinase 8 (Protein kinase K35) (predicted)
1372062_at	−0.703	−0.708	RGD1563395_predicted	similar to cyclin-dependent kinase 2-interacting protein (predicted)
1371517_at	−0.660	−0.627	RGD1566234_predicted	similar to Grb10 protein (predicted)
1377503_at	−0.558	−0.606	Riok2	RIO kinase 2 (yeast)
1387201_at	−0.766	−0.774	Rnf138	ring finger protein 138
1389258_at	−0.592	−0.653	Rnf138	ring finger protein 138
1376440_at	−0.741	−0.715	Rnf139_predicted	ring finger protein 139 (predicted)
1398572_at	−0.670	−0.547	Rnmt	RNA (guanine-7-) methyltransferase
1376065_at	−0.662	−0.617	Rrs1_predicted	RRS1 ribosome biogenesis regulator homolog (S. cerevisiae) (predicted)
1375441_at	−0.724	−0.680	Sars1	seryl-aminoacyl-tRNA synthetase 1
1374864_at	−0.370	−0.339	Spry2	sprouty homolog 2 (Drosophila)
1388967_at	−0.744	−0.714	Tcfe3_predicted	transcription factor E3 (predicted)
1388780_at	−0.683	−0.681	Terf2ip	telomeric repeat binding factor 2, interacting protein
1387450_at	−0.695	−0.708	Tgfa	transforming growth factor alpha
1370694_at	−0.858	−0.760	Trib3	tribbles homolog 3 (Drosophila)
1386321_s_at	−0.835	−0.676	Trib3	tribbles homolog 3 (Drosophila)
1370695_s_at	−0.831	−0.701	Trib3	tribbles homolog 3 (Drosophila)
1388868_at	−0.779	−0.736	Zfp216_predicted	zinc finger protein 216 (predicted)
Miscellaneous				
1385616_a_at	−0.734	−0.557	Asf1a_predicted	ASF1 anti-silencing function 1 homolog A (S. cerevisiae) (predicted)
1389569_at	−0.647	−0.578	Bxdc2	brix domain containing 2
1373196_at	−0.378	−0.414	Efha2	EF hand domain family, member A2
1372873_at	−0.599	−0.673	Fbxo38_predicted	F-box protein 38 (predicted)
1373836_at	−0.412	−0.503	Fyttd1	Forty-two-three domain containing 1
1374043_at	−0.379	−0.444	Gramd3	GRAM domain containing 3

Table 1. Continued.

Affymetrix probe ID	Correlation coefficient		Gene Symbol	Annotation
	Spearman's	Pearson's		
1390208_at	−0.586	−0.522	Htatip2_predicted	HIV-1 tat interactive protein 2, homolog (human) (predicted)
1371995_at	−0.802	−0.762	Klhl21_predicted	kelch-like 21 (Drosophila) (predicted)
1374879_x_at	−0.525	−0.490	Larp5_predicted	La ribonucleoprotein domain family, member 5 (predicted)
1388709_at	−0.683	−0.558	LOC362703	similar to WD-repeat protein 43
1384101_at	−0.682	−0.722	LOC682507	similar to Neural Wiskott-Aldrich syndrome protein (N-WASP)
1373761_at	−0.530	−0.535	LOC686611	similar to Protein FAM60A (Tera protein)
1373282_at	−0.596	−0.503	LOC686808	similar to mitochondrial carrier protein MGC4399
1372869_at	−0.554	−0.510	LOC689842	similar to Nucleolar GTP-binding protein 1 (Chronic renal failure gene protein) (GTP-binding protein NGB)
1373904_at	−0.749	−0.702	Lysmd2_predicted	LysM, putative peptidoglycan-binding, domain containing 2 (predicted)
1393239_at	−0.349	−0.462	Mtfr1_predicted	Mitochondrial fission regulator 1 (predicted)
1387950_at	−0.644	−0.629	Nip7	nuclear import 7 homolog (S. cerevisiae)
1373445_at	−0.732	−0.645	Nol8_predicted	nucleolar protein 8 (predicted)
1373737_at	−0.664	−0.674	ORF19	open reading frame 19
1376118_at	−0.603	−0.543	Otub2_predicted	OTU domain, ubiquitin aldehyde binding 2 (predicted)
1374438_at	−0.447	−0.460	Otud4	OTU domain containing 4
1374612_at	−0.669	−0.585	Papd5_predicted	PAP associated domain containing 5 (predicted)
1388355_at	−0.751	−0.650	Rbm17	RNA binding motif protein 17
1389065_at	−0.458	−0.498	Rbm34	RNA binding motif protein 34
1389228_at	−0.685	−0.607	RGD1304825_predicted	similar to RIKEN cDNA 2010309E21 (predicted)
1372185_at	−0.621	−0.634	RGD1306582	similar to RIKEN cDNA 2610205E22
1390392_at	−0.754	−0.718	RGD1309602_predicted	similar to RIKEN cDNA 2500001K11 (predicted)
1372329_at	−0.657	−0.627	RGD1311435	similar to hypothetical protein PRO0971
1373049_at	−0.492	−0.490	RGD1562136_predicted	similar to D1Ertd622e protein (predicted)
1388900_at	−0.719	−0.671	RGD1566118_predicted	RGD1566118 (predicted)
1372871_at	−0.717	−0.711	RGD735175	hypothetical protein MGC:72616
1375565_at	−0.513	−0.518	Timm22	translocase of inner mitochondrial membrane 22 homolog (yeast)
1390237_at	−0.573	−0.351	Timm8a	translocase of inner mitochondrial membrane 8 homolog a (yeast)
1373277_at	−0.624	−0.577	Tm2d3_predicted	TM2 domain containing 3 (predicted)
1374793_at	−0.518	−0.522	Wdr3_predicted	WD repeat domain 3 (predicted)
1371729_at	−0.473	−0.544	Ypel5	yippee-like 5 (Drosophila)
1390476_at	−0.740	−0.680	Zbtb39_predicted	Zinc finger and BTB domain containing 39 (predicted)
1373767_at	−0.634	−0.552	Zfand2a	zinc finger, AN1-type domain 2A

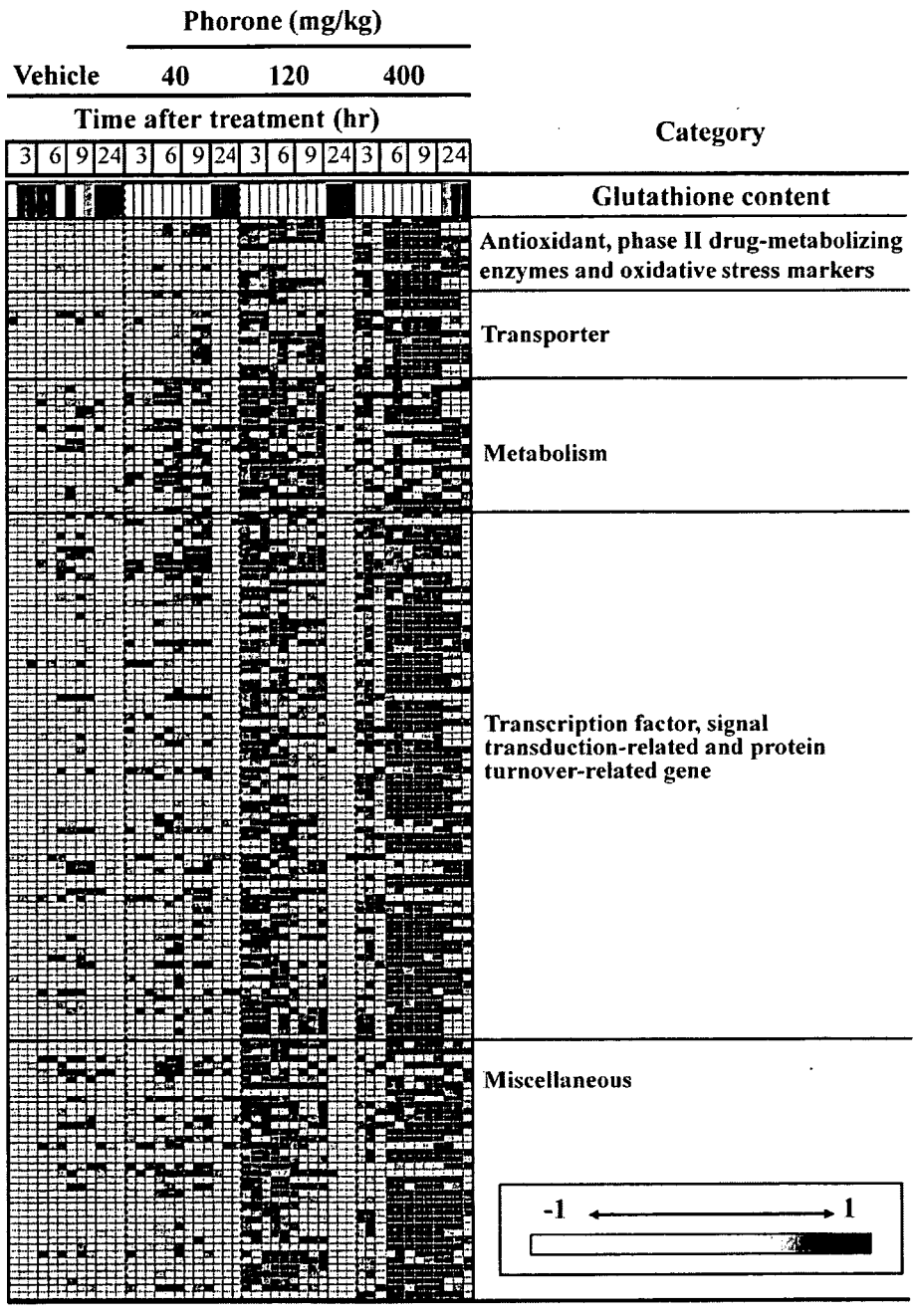

Fig. 3. Heat map representing glutathione content and gene expression level in rat liver treated with phorone.
Glutathione content and GeneChip signal data for GSH probe sets, obtained from rat livers treated with phorone or vehicle, are transformed to z-score by row, and are presented as a heat map where low and high scores are colored in white and black, respectively. Each row represents a probe set, and the vertical order of the probe sets is the same as that presented in Table 1. Each column represents individual rats treated either with phorone or vehicle.

Table 2. Plasma biochemistry and histopathological findings in rat liver treated with various prototypical hepatotoxicants.

Chemical	Dose (mg/kg)	Serum ALT activity (IU/L)		Serum AST activity (IU/L)		Histopathological findings observed in rat livers (number of animals)
		Control	Treated	Control	Treated	
Acetaminophen	1000	37.0 ± 3.1	51.0 ± 17.2	59.0 ± 6.3	76.4 ± 14.1*	Increased eosinophility of hepatocyte: central (3/5) Inflammatory infiltration: central (5/5)
Bromobenzene	300	50.8 ± 6.4	113.6 ± 49.9*	79.6 ± 7.0	481.0 ± 377.8	Hypertrophy, eosinophilic granular change (5/5) Cellular infiltration, centrilobular (5/5) Swelling, centrilobular (4/5) Necrosis, centrilobular (4/5)
Clofibrate	300	34.0 ± 5.5	38.0 ± 6.3	66.4 ± 8.0	79.0 ± 14.2	No findings
Chlorpromazine	45	32.4 ± 4.9	31.8 ± 1.8	62.2 ± 4.9	74.6 ± 8.4*	No findings
Glibenclamide	1000	32.2 ± 4.5	35.6 ± 2.9	61.4 ± 3.8	69.2 ± 4.7*	No findings
Methapyrilene	100	41.6 ± 9.5	68.4 ± 17.6*	71.8 ± 6.8	109.6 ± 25.7*	Single cell necrosis, hepatocyte (5/5) Hypertrophy, hepatocyte (5/5) Cellular infiltration, mononuclear cell, periportal (5/5) Anisoncleosis, hepatocyte (5/5)
Phenylbutazone	200	34.8 ± 4.8	49.4 ± 18.4	67.0 ± 6.3	76.6 ± 7.6	No findings
Aspirin	450	34.8 ± 5.3	44.2 ± 15.6	63.8 ± 4.5	75.6 ± 12.6	No findings
Carbon tetrachloride	300	37.2 ± 2.7	42.2 ± 4.6	66.6 ± 4.0	75.0 ± 13.3	Degeneration, hydropic: centrilobular (4/5) Cellular infiltration: centrilobular (3/5) Degeneration, fatty: centrilobular (4/5)
Coumarin	150	37.0 ± 3.9	40.2 ± 8.4	64.4 ± 8.6	85.8 ± 26.3	Hypertrophy, centrilobular (3/5)
Hexachlorobenzene	300	40.2 ± 8.7	47.0 ± 7.1	66.6 ± 3.3	69.2 ± 4.8	No findings
Perhexiline maleate	150	42.6 ± 5.9	50.0 ± 5.8	66.4 ± 5.1	71.6 ± 7.4	No findings
Thioacetamide	45	32.5 ± 3.4	137.2 ± 37.8**	63.5 ± 3.0	713.8 ± 542.6	Hypertrophy: centrilobular (5/5) Cellular infiltration, inflammatory (5/5) Change, eosinophilic hepatocyte (5/5) Necrosis, centrilobular (5/5)

Rat groups consisting of 5 animals were administered with the compounds listed in the table and euthanized 24 hr after treatment. Both blood chemistry and histopathology data are summarized using the 5 rats. Note that microarray analysis was conducted using 3 rats out of the 5. The data are presented as mean ±S.D. * and **, $p<0.05$ and $p<0.01$, respectively, determined by two-sample *t*-test.

hexachlorobenzene or perhexiline maleate did not show any histopathological changes.

Gene expression analysis for rat liver treated with various hepatotoxicants

PCA was performed using GSH probe sets for GeneChip data obtained from rat livers 24 hr after treatment with various prototypical hepatotoxicants (Fig. 4). It was obvious from the figure that a few compounds were distributed to the direction of the first principal component (PC 1) with relatively high contribution (57.6%), i.e., 300 mg/kg bromobenzene, 150 mg/kg coumarin, 1000 mg/kg acetaminophen, and 45 mg/kg thioacetamide, in that order. Rats treated with other chemicals or corresponding vehicles showed no apparent shift toward the PC 1 axis, but showed dispersed distributions along the PC 2 axis.

Glutathione content in rat livers treated with bromobenzene

From PCA using GSH probe sets, we found that bromobenzene was the most potent GSH-depletor among the compounds tested. In order to confirm this, hepatic glutathione content in the liver treated with this compound was actually quantified. It was found that the contents were significantly reduced 3, 6 and 9 hr after 300 mg/kg bromobenzene treatment (Fig. 5). It appeared that some of the treated rats showed recovery or rather rebound of GSH contents 24 hr after treatment since the mean value recovered to the control level with large variance.

Time-course of gene expression profile in rat liver treated with bromobenzene

In order to analyze the time dependent correlation between GSH contents and gene expression changes, PCA was performed by adding the data of 3, 6, and 9 hr after bromobenzene treatment to the same

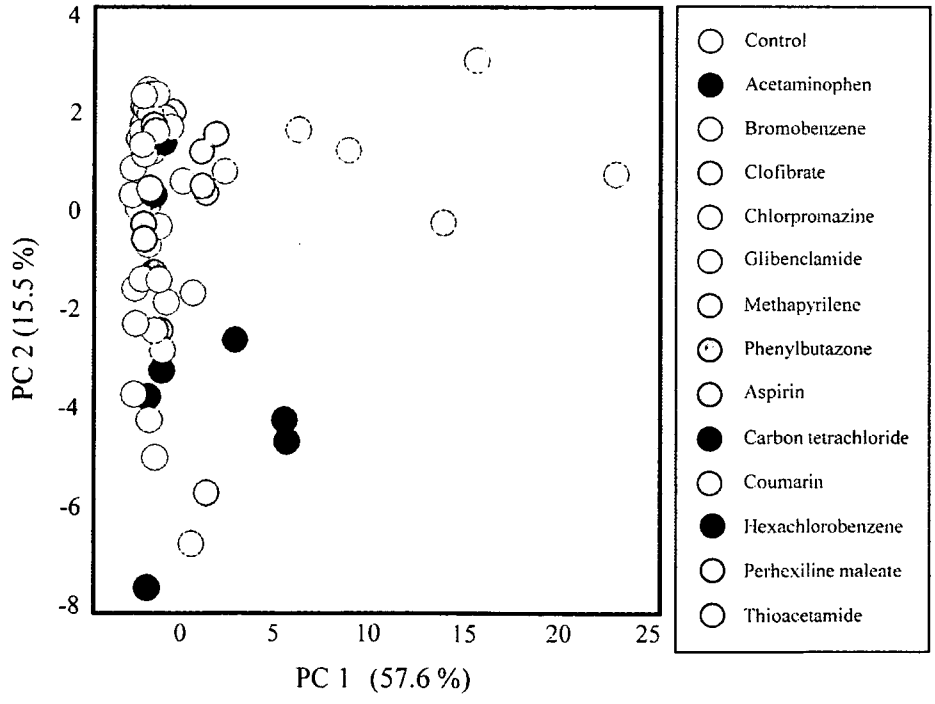

Fig. 4. PCA for GeneChip data of rat liver 24 hr after treatment with various hepatotoxicants.
PCA was performed using GSH probe sets for GeneChip data of rat livers 24 hr after treatment with various hepatotoxicants. Each spot, colored by chemical type, represents individual samples. Bromobenzene, coumarin, and acetaminophen showed apparent shift from control, suggesting a perturbation of glutathione homeostasis in the liver after treatment.

data in Fig. 4. Fig. 6 shows that signal profiles of GSH probe sets did not apparently differ from those of controls, 3 and 6 hr after 300 mg/kg bromobenzene treatment. After 9 hr, they shifted away toward both PC1 and PC2 axis, approaching the position of 24 hr on PC1 axis.

DISCUSSION

Hepatic total glutathione content was significantly decreased in all the phorone-treated groups 3 hr after treatment (Fig. 2). After acute glutathione depletion, the hepatic glutathione content gradually recovered from 6 hr in the phorone-treated group (40 and 120 mg/kg), resulting in a significantly higher glutathione content, compared to the vehicle-treated rats 24 hr after treatment. Plasma ALT activity was elevated from 9 hr after 400 mg/kg phorone treatment, suggesting slight hepatocellular injury. Since secondary undesirable effects caused by slight hepatotoxicity (other than glutathione depletion) might affect the gene expression profile, we excluded GeneChip data of the 400 mg/kg phorone-treated rats from analysis for identification of the glutathione depletion-responsive gene probe sets. Previously, candidate marker genes whose mRNA levels were inversely correlated with hepatic glutathione content were identified using L-buthionine-[S,R]-sulfoximine (BSO) as a glutathione-depleting agent (Kiyosawa *et al.*, 2004). In the present study, we used phorone as a glutathione-depleting agent instead of BSO. We identified a total of 161 probe sets, referred to as 'GSH probe sets', whose signal showed

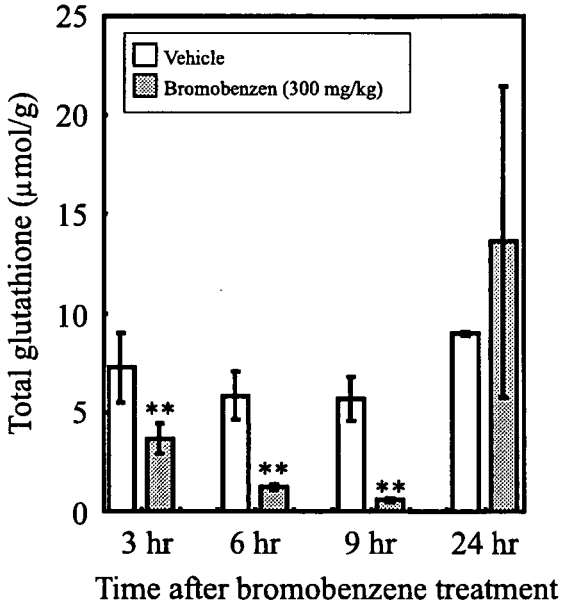

Fig. 5. Glutathione content in rat liver treated with bromobenzene.
Three rats per group were treated with 300 mg/kg bromobenzene or vehicle, and the livers were removed 3, 6, 9 and 24 hr after treatment. Hepatic glutathione content (total) was measured and the data are presented as mean ± S.D. Hepatic glutathione content was significantly decreased 3, 6 and 9 hr after bromobenzene treatment, and recovered 24 hr after treatment, although the glutathione level showed a high variability at this time point. **, $p<0.01$ determined by two-sample *t*-test.

an inverse correlation with hepatic glutathione content.

The present study had two advantages compared with the BSO study previously reported. First, the glutathione-depleting mechanism differs from phorone (a reactor to GSH thiol) and BSO (an inhibitor of gamma-glutamylcysteine synthetase). Comparing the two glutathione-depleting mechanisms, the phorone-induced one is thought to be more similar to drug-induced glutathione depletion (as in the acetaminophen overdose-induced one) where hepatic glutathione is depleted by elevated elimination, not by inhibition of glutathione synthesis. Second, the present study set multiple dose ranges and time points. The total number of rats tested in the phorone study was 36 (twelve 400 mg/kg phorone-treated rats were excluded from the gene selection procedure), whereas the previous BSO study used only 8 rats (Kiyosawa *et al.*, 2004). Thus, the GSH probe sets identified in the present study would give us more reliable information for evaluation of the potential risk of drug-induced glutathione depletion.

The GSH probe sets contained antioxidant/phase II drug-metabolizing enzymes, oxidative stress markers, transporters, metabolism-related genes, transcription factors and signal transduction-related genes, and others. GSH probe sets contain a modifier subunit of glutamate cysteine ligase gene, which encodes a key enzyme for glutathione synthesis (Moinova and Mulcahy, 1999). In addition, a prototypical oxidative stress-responsive gene, heme oxygenase I, which is reported to be regulated by oxidative stress sensor Nrf2 (Nguyen *et al.*, 2003), was identified as GSH probe sets. Furthermore, several genes were found to be in common with previously reported gene sets identified from the BSO-induced glutathione depletion model rat, such as GTP cyclohydrolase I and HMG-CoA reductase (Kiyosawa *et al.*, 2004). On the other hand, a

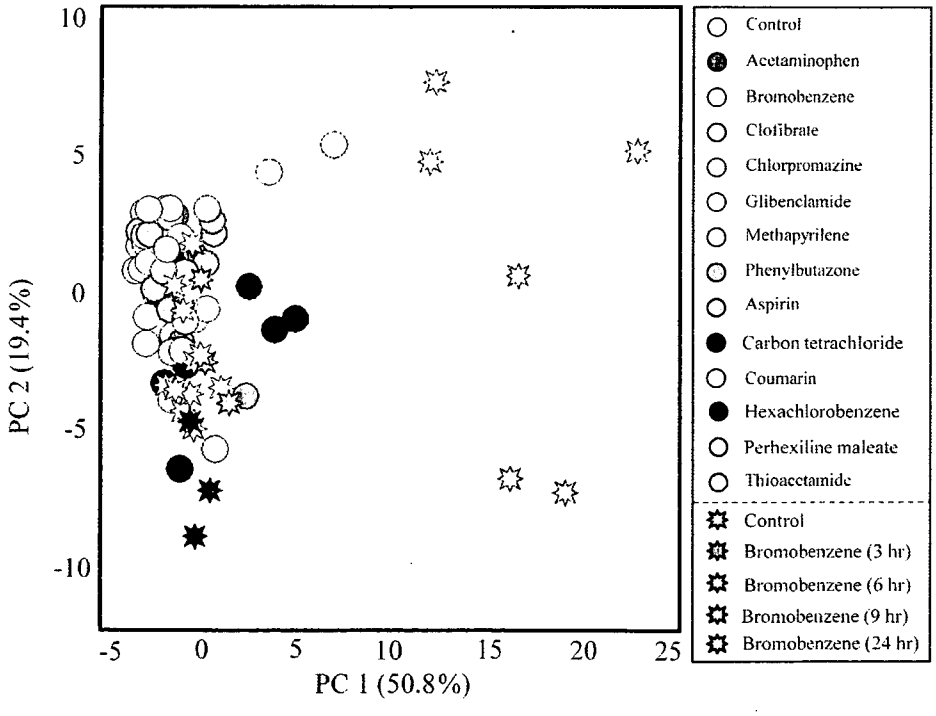

Fig. 6. Time-course of gene expression profile in rat liver treated with bromobenzene.
PCA was performed using GSH probe sets for GeneChip data of rat livers 3, 6, 9 and 24 hr after 300 mg/kg bromobenzene treatment, as well as those 24 hr after treatment with hepatotoxicants, which are the same as those shown in Fig. 4. Each spot colored by chemical types represents individual samples. Gene expression profiles of rats treated with bromobenzene did not show an apparent shift away from corresponding controls 3 and 6 hr after treatment. Those 9 and 24 hr after treatment showed an apparent shift from the controls.